

## Research Article

An Atoms-in-Molecules Analysis of the Structure of Di-*n*-Butyltin(IV) Derivative of Glycylphenylalanine

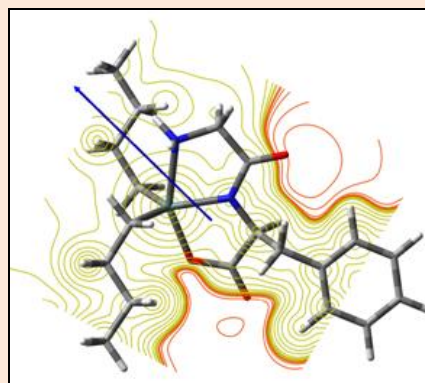
Sandeep Pokharia\*

Organometallics and Molecular Modeling Group, Chemistry Section, M.M.V., Banaras Hindu University, Varanasi, India

**Abstract**

The topological and energetic properties of the electron density distribution  $\rho(\vec{r})$  for the tin-ligand interaction in *n*-Bu<sub>2</sub>SnL (where, L is the dianion of glycylphenylalanine), the geometric configuration of which was optimized at B3LYP/6-31G(d,p)/LANL2DZ(Sn) level of theory, have been theoretically calculated at the bonds around the central Sn atom in terms of atoms-in-molecules (AIM) theory using AIMAll (Version 16.01.09, standard). In *n*-Bu<sub>2</sub>SnL, the formation of a (3,−1) critical point in the internuclear region between tin atom and bonded/coordinated atoms provided an evidence of a bonding interatomic interaction, and calculated bond path angles indicated a distorted trigonal bipyramidal geometry. The calculated topological and energetic parameters suggested a weak closed-shell interaction in all the bonded/coordinated bonds to Sn atom, which indicated a coordination (non-sharing) bonding character in Sn–ligand bonding. The calculated atomic charges suggested negatively charged centers around the central Sn atom.

**Keywords:** AIM, DFT, di-*n*-butyltin(IV), glycylphenylalanine, topological parameters

**\*Correspondence**

Author: Sandeep Pokharia  
Email: sandeep@bhu.ac.in

**Introduction**

In recent years, the chemistry of organotin(IV) complexes has witnessed a great interest, owing to their structural diversity and wide range of industrial and biological applications [1]. These complexes exhibit expanded coordination upon inter- or intra-molecular interaction with hetero donor atoms owing to the low lying empty 5d atomic orbitals and pronounced electron-acceptor ability of the Sn atoms, thus making them suitable for the design of newer materials with unique structural features [2]. Further, these complexes are found to possess antiproliferative activity, which is dependent on the nature of coordinated bonds with the central Sn atom. Accordingly, several organotin(IV) complexes of dipeptides have been modelled for metal-protein interactions and also been shown to exhibit wide range of biological activities [3-5]. These organotin(IV) complexes of dipeptides possess unique structural and geometrical features such as, interaction through hetero donor atoms (N/O) as-well-as existence of a distorted geometrical configuration around the central Sn atom. Thus, a thorough study of the electronic structure of these complexes is indispensable in order to formulate a theoretical basis of these structural features.

In the contemporary research, the atoms-in-molecules (AIM) methodology is frequently used in the modeling of the electron density distribution  $\rho(\vec{r})$  in intermolecular interactions [6]. The topological properties of  $\rho(\vec{r})$  have been well established for many molecular systems involving organotin(IV) complexes with hetero donor atoms [7-10], but the studies on the nature of tin-ligand bond in organotin(IV)-peptide complexes is rarely available. Hence, in order to understand the nature of coordinated bonds, a systematic study has been initiated on the topological analysis of organotin(IV)-peptide system. The present study attempts to delineate the topological and energetic features of  $\rho(\vec{r})$  using AIM theory, in the coordinated bonds in di-*n*-butyltin(IV) derivative (*n*-Bu<sub>2</sub>SnL) of glycylphenylalanine (H<sub>2</sub>L), a dipeptide containing an aromatic side chain at C-terminal residue.

## Computational Details

The nature of coordinated bonds in *n*-Bu<sub>2</sub>SnL has been interpreted in terms of AIM theory using AIMSum component of AIMAll software package [11]. The wavefunction input for AIM analysis has been generated from the previously optimized geometrical configuration of *n*-Bu<sub>2</sub>SnL at B3LYP/6-31G(d,p)/LANL2DZ(Sn) level of theory using the Gaussian 09 program package [12]. The topological and energetic analysis of  $\rho(\vec{r})$  has been carried out in terms of (3,-1) critical points (bond critical points) and (3,+1) critical points (ring critical points) around the central Sn atom in *n*-Bu<sub>2</sub>SnL derivative. The topological and energetic parameters obtained at the bond critical points (BCPs) are the electron density ( $\rho(\vec{r})$ ), the Laplacian of the electron density ( $\nabla^2\rho(\vec{r})$ ), the principal curvature of  $\rho(\vec{r})$  in the normal plane to the bond path direction ( $\lambda_{1CP}$  and  $\lambda_{2CP}$ ), the principal curvature along the bond path direction ( $\lambda_{3CP}$ ), bond ellipticity ( $\epsilon$ ), the electron kinetic ( $G(\vec{r})$ ), potential ( $V(\vec{r})$ ) and total ( $H(\vec{r})$ ) energy densities. The atomic characteristics such as, atomic volume and atomic charge at the selected atoms, and bond path angles for a group of atoms has also been calculated in *n*-Bu<sub>2</sub>SnL derivative. The geometric configuration of *n*-Bu<sub>2</sub>SnL has been interpreted in terms of calculated bond path angles for a selected group of atoms around the central Sn atom.

## Results and Discussion

The values of electron density distribution  $\rho(\vec{r})$  were calculated on the ground state optimized geometry in gas phase of *n*-Bu<sub>2</sub>SnL derivative of glycylphenylalanine (H<sub>2</sub>L) at the B3LYP/6-31G(d,p)/LANL2DZ(Sn) level of theory, and then  $\rho(\vec{r})$  was analyzed within the framework of the AIM theory. The structure of *n*-Bu<sub>2</sub>SnL along with the atom number notation and the ground state optimized geometry used for wavefunction calculation for AIM analysis is represented in **Figure 1**. As evident from the Figure 1(b), the *n*-Bu<sub>2</sub>SnL complex adopts a trigonal bipyramidal arrangement around the central Sn atom with two *n*-butyl groups and a deprotonated peptide nitrogen (N<sub>peptide</sub>) occupying the equatorial positions, and terminal amino nitrogen (N<sub>amino</sub>) and the deprotonated carboxylic oxygen (O<sub>carboxyl</sub>) in the axial positions. Thus, the insight into this intermolecular interaction of hetero donor atoms in H<sub>2</sub>L with *n*-Bu<sub>2</sub>Sn(IV) moiety was obtained from the full topological and energetic analysis of the  $\rho(\vec{r})$  at these selected BCPs around the central Sn atom in *n*-Bu<sub>2</sub>SnL derivative. The formation of a (3,-1) critical point in the internuclear region between the central Sn atom and bonded/coordinated atoms in the trigonal bipyramidal arrangement around it provided the evidence of a bonding interatomic interaction through the topological analysis of  $\rho(\vec{r})$ . The bond path corresponding to these critical points link the BCP with two (3,-3) critical points located at the coordinated/bonded atoms and the central Sn atom, thus providing an evidence that, in terms of AIM theory, the group of atoms are bonded to one another [13]. The values of selected AIM topological parameters at these selected BCPs are presented in **Table 1**.

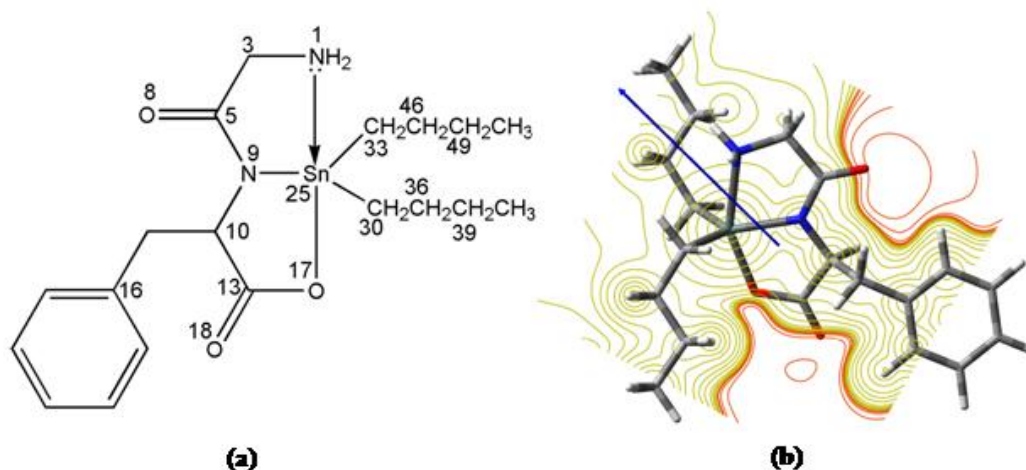


**Figure 1** (a) Structure of *n*-Bu<sub>2</sub>SnL along with the atom number notation, and (b) Ground state optimized geometry of *n*-Bu<sub>2</sub>SnL at B3LYP/6-31G(d,p)/LANL2DZ(Sn) level of theory used for the generation of wavefunction for calculation of topological and energetic parameters in AIM analysis

**Table 1** Topological and energetic properties of  $\rho(\vec{r})$  calculated at the (3,-1) and (3,+1) critical point of the selected bonded interactions in *n*-Bu<sub>2</sub>SnL derivative of glycyphenylalanine (H<sub>2</sub>L) at B3LYP/6-31G(d,p)/LANL2DZ(Sn) level of theory<sup>a</sup>

Type <sup>b</sup>	$\rho(\vec{r})^c$	$\nabla^2\rho(\vec{r})^d$	$\lambda_{1CP}^e$	$\lambda_{2CP}$	$\lambda_{3CP}$	$\epsilon^f$	$G(\vec{r})^g$	$V(\vec{r})^h$	$H(\vec{r})^i$	$ V(\vec{r})/G(\vec{r}) $	$H(\vec{r})/\rho(\vec{r})^j$	$-\lambda_{1CP}/\lambda_{3CP}$
<b>(3,-1) critical point or Bond critical point (BCP)</b>												
Sn-N1	0.046	0.182	-0.047	-0.046	0.276	0.011	0.017	-0.023	-0.0061	1.353	-0.133	0.171
Sn-N9	0.110	0.448	-0.163	-0.145	0.755	0.127	0.041	-0.070	-0.0286	1.693	-0.636	0.216
Sn-O17	0.109	0.585	-0.170	-0.162	0.917	0.050	0.055	-0.072	-0.0169	1.309	-0.155	0.185
Sn-C30	0.107	0.193	-0.128	-0.126	0.447	0.022	0.021	-0.064	-0.0433	3.104	-0.406	0.287
Sn-C33	0.106	0.193	-0.128	-0.125	0.446	0.031	0.021	-0.064	-0.0432	3.089	-0.406	0.288
<b>(3,+1) critical point or Ring critical point (RCP)</b>												
N1-C3-	0.021	0.109	-0.015	0.030	0.094	-	0.023	-0.019	0.0042	0.817	0.205	0.159
C5-												
N9-Sn29												
N9-C10-	0.025	0.137	-0.020	0.049	0.108	-	0.029	-0.025	0.0043	0.853	0.174	0.183
C13-												
O17-Sn29												
O17-Sn29-	0.006	0.025	-0.004	0.010	0.019	-	0.005	-0.004	0.001	0.759	0.197	0.215
C30-												
C36-C39-												
H40												
N1-H2-	0.005	0.018	-0.001	0.006	0.014	-	0.004	-0.003	0.001	0.785	0.175	0.084
H50-												
C49-C46-												
C33-Sn29												

<sup>a</sup>All the values are in atomic units; <sup>b</sup>Atom number as represented in Figure 1(a); <sup>c</sup>Electron density distribution at the critical point (CP); <sup>d</sup>Laplacian of the electron density at CP; <sup>e</sup> $\lambda_{iCP}$  ( $i = 1,2,3$ ) are the eigenvalues of the Hessian of  $\rho(\vec{r})$  in ascending order, where  $\lambda_{1CP}$  and  $\lambda_{2CP}$  are the principal curvature of  $\rho(\vec{r})$  in the normal plane to the bond path direction and  $\lambda_{3CP}$  is the principal curvature along the bond path direction; <sup>f</sup>Bond ellipticity =  $[(\lambda_{1CP}/\lambda_{2CP}) - 1]$ ; <sup>g</sup>Lagrangian form of kinetic energy density; <sup>h</sup>Potential energy density; <sup>i</sup>Total energy density =  $G(\vec{r}) + V(\vec{r})$ ; <sup>j</sup>Bond degree parameter.

At the critical point in the internuclear region, the magnitude of  $\rho(\vec{r})$  measures the strength of interaction between the involved nuclei, and thus greater the value of  $\rho(\vec{r})$  stronger will be the interaction [14]. Further, the interaction between the involved atoms can be characterized by the topological properties of  $\rho(\vec{r})$  at the critical point, and hence according to the AIM methodology the classification of this interaction is defined by the sign of the Laplacian  $\nabla^2\rho(\vec{r})$ . Therefore, the strong shared-shell (SS-) interatomic interaction is evidenced by a local concentration of the electron density distribution at the critical point when  $\nabla^2\rho(\vec{r}) < 0$ , whereas the weak closed-shell (CS-) interaction exhibit its local depletion when  $\nabla^2\rho(\vec{r}) > 0$ . As evident from the results (Table 1), the small value of  $\rho(\vec{r})$  and the positive Laplacian  $\nabla^2\rho(\vec{r})$ , suggests a contraction of an electron charge away from the interatomic region between the bonded atom and the Sn atom. According to the  $\rho(\vec{r})$  values (Table 1), the bond strength around the central Sn atom is in the order: Sn-N1<sub>(amino)</sub> < Sn-C33<sub>( $\alpha$ )</sub> < Sn-C30<sub>( $\alpha$ )</sub> < Sn-O17<sub>(carboxyl)</sub> < Sn-N9<sub>(peptide)</sub>.

However, the value of  $\rho(\vec{r})$  for Sn-N<sub>peptide</sub> and Sn-O<sub>carboxylic</sub> is close, whereas that for Sn-N<sub>amino</sub> is much smaller to that of covalent Sn-C bonds, indicating small  $d_{N(peptide)-Sn}$  and  $d_{O(carboxylate)-Sn}$ , and large  $d_{N(amino)-Sn}$ , owing to the fact that strength of the interaction of deprotonated N<sub>peptide</sub> and O<sub>carboxylate</sub> is major in comparison to that of N<sub>amino</sub>. The positive values of  $\nabla^2\rho(\vec{r})$  were often found at the BCP between atoms involved in the dative bonds, including the intramolecular N→Sn [7], and O→Sn [9] bonds. The magnitude of the curvature or eigenvalue of the Hessian of  $\rho(\vec{r})$  in an atomic surface  $\lambda_{1CP}$  and  $\lambda_{2CP}$  (where,  $\lambda_1$  and  $\lambda_2$  are the curvatures of  $\rho(\vec{r})$  at BCP directed along axes perpendicular to the bond path) are negative, which indicates that the charge density attains its maximum value at the BCP, whereas along a bond path  $\lambda_{3CP}$  is positive, which indicates that the charge density attains its minimum value at the BCP, a behavior at the BCP around the central Sn atom in *n*-Bu<sub>2</sub>SnL which is in accordance to the fact put forwarded earlier [6]. Further, as evident from the results (Table 1), all the bonds in the coordination sphere around the central Sn atom involves weak CS-interaction as the magnitude of the ratio of the perpendicular contractions of

$\rho(\vec{r})$  to its parallel expansion i.e.,  $|\lambda_{1CP}/\lambda_{3CP}| < 1$  (where,  $\lambda_{1CP}$  and  $\lambda_{3CP}$  are the lowest and highest eigenvalues of the Hessian matrix of  $\rho(\vec{r})$ ) [6,14]. Furthermore, the stability of a bond can be measured in terms of bond ellipticity,  $\varepsilon = [\lambda_{1CP}/\lambda_{2CP} - 1]$ , which provides a measure of the extent to which charge is preferentially accumulated in a given plane, and a high  $\varepsilon$  value indicates an unstable bond [6]. The order of  $\varepsilon$  (Table 1), for BCPs in the coordination sphere around the central Sn atom is:  $\text{Sn}-\text{N}_{\text{peptide}} > \text{Sn}-\text{O}_{\text{carboxyl}} > \text{Sn}-\text{C}_{\alpha'} > \text{Sn}-\text{C}_{\alpha} > \text{Sn}-\text{N}_{\text{amino}}$ , which indicates that the interaction of hetero donor atoms in the ligand ( $\text{H}_2\text{L}$ ) results in a weaker bond except  $\text{Sn}-\text{N}_{\text{amino}}$  in comparison to the covalently bonded carbon atoms of the two *n*-butyl groups in the *n*- $\text{Bu}_2\text{SnL}$  derivative.

The AIM energetic parameters at the selected BCPs are also presented in Table 1. For all the selected BCPs around the central Sn atom, the  $G(\vec{r})$  is less than  $V(\vec{r})$  resulting in the negative sign of the total electron energy density  $H(\vec{r}) (= G(\vec{r}) + V(\vec{r}))$ . The sign of  $H(\vec{r})$  has been suggested as one of the sufficient condition ( $H(\vec{r}) < 0$ ) apart from the existence of a (3,-1) critical point in the internuclear region (a necessary condition), for a covalent bond even though a CS-interaction is involved [14]. Since, the value of  $H(\vec{r}) < 0$ , thus,  $\text{Sn}-\text{N}_{\text{amino}}$ ,  $\text{Sn}-\text{O}_{\text{carboxyl}}$ ,  $\text{Sn}-\text{N}_{\text{peptide}}$ ,  $\text{Sn}-\text{C}_{\alpha}$  and  $\text{Sn}-\text{C}_{\alpha'}$  bonds possess a covalent character. Further,  $V(\vec{r})$  and  $G(\vec{r})$  are interpreted as the pressures exerted on and by the electrons at the critical point, and hence the ratio  $|V(\vec{r})/G(\vec{r})| > 1$  for  $\text{Sn}-\text{N}_{\text{peptide}}$ ,  $\text{Sn}-\text{N}_{\text{amino}}$ ,  $\text{Sn}-\text{O}_{\text{carboxyl}}$ ,  $\text{Sn}-\text{C}_{\alpha}$  and  $\text{Sn}-\text{C}_{\alpha'}$  indicates that these interactions are stabilized by a local concentration of the charge [6, 14]. For the internuclear distances exhibiting a stable bonding molecular orbital configuration ( $d < d_{\text{cov}}$ ), the bond degree ( $\text{BD} = H(\vec{r})/\rho(\vec{r})$ ) gives the total energy per electron at the BCP [14]. Hence, a parameter covalence degree (CD) can be quantitatively assigned to any pairwise interaction, i.e.,  $\text{BD} = \text{CD}$  when  $H(\vec{r})/\rho(\vec{r}) < 0$ , and thus, stronger the interaction greater will be the CD magnitude. Similarly, an index of non-covalent interactions quantifying a softening degree (SD) per electron density unit at the BCP is defined for  $d > d_{\text{cov}}$  ( $H(\vec{r})/\rho(\vec{r}) > 0$ ), and thus, weaker the interaction greater will be the SD magnitude. The magnitude of  $H(\vec{r})/\rho(\vec{r})$  (Table 1) indicates a strong interaction quantifying a covalence degree in  $\text{Sn}-\text{N}_{\text{amino}}$ ,  $\text{Sn}-\text{N}_{\text{peptide}}$ ,  $\text{Sn}-\text{O}_{\text{carboxyl}}$ ,  $\text{Sn}-\text{C}_{\alpha}$  and  $\text{Sn}-\text{C}_{\alpha'}$  bonds.

Apart from the BCP analysis around the central Sn atom in *n*- $\text{Bu}_2\text{SnL}$ , its structure is further analyzed in terms of (3,+1) critical points (RCPs). The number of RCPs formed in *n*- $\text{Bu}_2\text{SnL}$  is nine, and Poincare-Hopf relationship is also satisfied [11]. The topological and energetic parameters for four RCPs viz., N1-C3-C5-N9-Sn29 (R1), N9-C10-C13-O17-Sn29 (R2), O17-Sn29-C30-C36-C39-H40 (R3) and N1-H2-H50-C49-C46-C33-Sn29 (R4) are presented in Table 1. Of these the RCPs viz. R1 and R2 constitute the bipyramidal arrangement above and below the trigonal plane, thus establishing that *n*- $\text{Bu}_2\text{SnL}$  adopts a trigonal bipyramidal arrangement around the central Sn atom. Also, the calculated values of  $\rho(\vec{r})$ , the Laplacian  $\nabla^2\rho(\vec{r})$  and  $H(\vec{r})$  indicates a weaker CS-interaction between the involved atoms.

**Table 2** Atomic charge (a.u.) and atomic volume (bohr<sup>3</sup>) at the selected atoms, and bond path angles (°) at the selected group of atoms in *n*- $\text{Bu}_2\text{SnL}$  at B3LYP/6-31G(d,p)/LANL2DZ(Sn) level of theory

Atom Characteristics			Bond Path Angle	
Atom <sup>a</sup>	Net charge	Volume	A-B-C	Angle
Sn	1.895	111.6	N9-Sn-N1	73.17
C30	-0.336	79.9	O17-Sn-N1	152.88
C33	-0.335	82.5	O17-Sn-N9	79.76
N1	-1.134	97.6	C30-Sn-N1	86.82
N9	-1.353	101.0	C30-Sn-N9	119.17
O17	-1.224	125.2	C30-Sn-O17	105.49
C3	0.348	59.8	C33-Sn-N1	95.78
C5	1.562	40.8	C33-Sn-N9	121.56
C10	0.375	45.6	C33-Sn-O17	99.62
C13	1.684	37.9	C33-Sn-C30	117.11
O8	-1.231	148.4		
O18	-1.231	150.6		

<sup>a</sup>Atom number as represented in Figure 1(a)

The atomic charges and atomic volumes at the all the atoms of *n*-Bu<sub>2</sub>SnL have been also calculated using AIM theory, and the results for the selected atoms are presented in Table 2. As evident from the results, relative to the positively charged Sn atom in *n*-Bu<sub>2</sub>SnL all the atoms bonded to it bear negative charge, which further confirms a partial transfer of charge density towards these atoms indicative of an ionic interaction in them. The evidence for a distorted trigonal bipyramidal arrangement is further obtained from the calculated bond path angles around the central Sn atom (Table 2).

### Conclusion

The present study calculates the topological and energetic parameters at the bond critical points on the basis of atoms-in-molecules theory and hence highlights the features of tin-ligand bonds in di-*n*-butyltin(IV) complex of glycylphenylalanine. The study demonstrates that all metal-ligand bonds in *n*-Bu<sub>2</sub>SnL have coordination (non-sharing) bonding character. Further, the geometric parameters suggest a distorted trigonal bipyramidal arrangement around the central Sn atom. Most significantly, the study signifies the importance of AIM theory in understanding the structural features and nature of bonding in diorganotin(IV)-dipeptide system.

### Acknowledgements

The author is thankful to Banaras Hindu University, Varanasi for providing necessary infrastructural and computational facilities. Thanks are also due to Dr. Hirdyesh Mishra, Physics Section, M.M.V., B.H.U., Varanasi for providing access to the Gaussian09 software package.

### References

- [1] Nath M, Appl Organometal Chem 2008, 22, 598-612.
- [2] Pellerito L, Nagy L, Coord Chem Rev 2002, 224, 111-150.
- [3] Katsoulakou E, Tiliakos M, Papaefstathiou G, Terzis A, Raptopoulou C, Geromichalos G, Papazisis K, Papi R, Pantazaki A, Kyriakidis D, Cordopatis P, Manessi-Zoupa E, J Inorg Biochem 2008, 102, 1397-1405.
- [4] Nath M, Singh H, Kumar P, Kumar A, Song X, Eng G, Appl Organometal Chem 2009, 23, 347-358.
- [5] Girasolo MA, Rubino S, Portanova P, Calvaruso G, Ruisi G, Stocco G, J Organomet Chem 2010, 695, 609-618.
- [6] Bader RFW, Chem Rev 1991, 91, 893-928.
- [7] Karlov SS, Tyurin DA, Zabalov MV, Churakov AV, Zaitseva GS, J Mol Struct 2005, 724, 31-37.
- [8] Naseh M, Sedagat T, Tarassoli A, Shakerzadeh E, Comput Theor Chem 2013, 1005, 53-57.
- [9] Korlyukov AA, Lyssenko KA, Baukov YI, Bylikin SY, J Mol Struct 2013, 1051, 49-55.
- [10] Matczak P, Struct Chem 2015, 26, 301-318.
- [11] AIMAll (Version 16.01.09, standard), T.A. Keith, TK Gristmill software, Overland Park KS, USA, 2016 (<http://aim.tkgristmill.com>).
- [12] Frisch MJ, Trucks GW, Schlegel HB, Scuseria GE, Robb MA, Cheeseman JR, Scalmani G, Barone V, Mennucci B, Petersson GA, Nakatsuji H, Caricato M, Li X, Hratchian HP, Izmaylov AF, Bloino J, Zheng G, Sonnenberg JL, Hada M, Ehara M, Toyota K, Fukuda R, Hasegawa J, Ishida M, Nakajima T, Honda Y, Kitao O, Nakai H, Vreven T, Montgomery JAJr, Peralta JE, Ogliaro F, Bearpark M, Heyd JJ, Brothers E, Kudin KN, Staroverov VN, Keith T, Kobayashi R, Normand J, Raghavachari K, Rendell A, Burant JC, Iyengar SS, Tomasi J, Cossi M, Rega N, Millam JM, Klene M, Knox JE, Cross JB, Bakken V, Adamo C, Jaramillo J, Gomperts R, Stratmann RE, Yazyev O, Austin AJ, Cammi R, Pomelli C, Ochterski JW, Martin RL, Morokuma K, Zakrzewski VG, Voth GA, Salvador P, Dannenberg JJ, Dapprich S, Daniels AD, Farkas O, Foresman JB, Ortiz JV, Cioslowski J, Fox DJ, Gaussian09, Revision B.01; Gaussian, Inc., Wallingford CT, 2010.
- [13] Bader RFW, J Phys Chem 1998, 102, 7314-7323.
- [14] Espinosa E, Alkorta I, Elguero J, Molins E, J Chem Phys 2002, 117, 5529-5542.

© 2016, by the Authors. The articles published from this journal are distributed to the public under "Creative Commons Attribution License" (<http://creativecommons.org/licenses/by/3.0/>). Therefore, upon proper citation of the original work, all the articles can be used without any restriction or can be distributed in any medium in any form.

### Publication History

Received 09<sup>th</sup> Mar 2016  
Accepted 28<sup>th</sup> Apr 2016  
Online 20<sup>th</sup> Oct 2016